Engenharia Agrícola

ISSN: 1809-4430 (on-line)

www.engenhariaagricola.org.br

Doi: http://dx.doi.org/10.1590/1809-4430-Eng.Agric.v39nep13-22/2019

Special Issue: Precision Agriculture

DELIMITATION OF HOMOGENEOUS ZONES IN VINEYARDS USING GEOSTATISTICS AND MULTIVARIATE ANALYSIS OF DIFFERENT VEGETATION INDICES

Bruno R. S. Costa[1], Henrique Oldoni[1], Romero C. Rocha Junior[2], Luís H. Bassoi[3*]

[3*]Correponding author. Embrapa Instrumentação/ São Carlos - SP, Brasil.
E-mail: luis.bassoi@embrapa.br | ORCID ID: https://orcid.org/0000-0001-9469-8953

KEYWORDS

Vitis vinifera L., canopy density, agricultural instrumentation.

ABSTRACT

Vegetation indices (VIs) are quantitative measures used to describe the distribution and spatial variability of the vegetation cover of natural or cultivated areas. The aim of this study was to delimit homogeneous zones (HZs) of different VIs using geostatistics and multivariate analysis in order to identify vegetation patterns in Cabernet Franc and Cabernet Sauvignon vineyards. The evaluation was performed in two vineyards in the municipality of Espírito Santo do Pinhal in the state of São Paulo, Brazil. Reflectance (ρ) was measured at three wavelengths of the electromagnetic spectrum (670, 730, and 780 nm) at canopy height in georeferenced points along planting rows using the Crop Circle ACS-430 active sensor. Nine VIs were calculated based on the ratios between the ρ values. Geostatistical data analysis allowed the spatial prediction of VIs by ordinary kriging interpolation. Principal component analysis and fuzzy k-means clustering were applied for HZs delimitation and the optimal number of zones was defined according to cluster validity functions. Despite the variations of the VIs spatial distribution patterns, the multivariate analysis resulted in a representative categorization of the grapevine vegetative vigor and delimitation of HZs for this characteristic. This was validated according to the observed significant differences between VIs.

INTRODUCTION

Vegetation indices (VIs) are calculated as ratios of reflectance measurements in different spectral bands, particularly the visible and near-infrared bands, of part of the solar radiation that interacts with leaves that compose a plant canopy. They are traditionally used in remote sensing to evaluate the current state of vegetation, taking advantage of differences in reflectance patterns between vegetation and other surfaces (Payero et al., 2004).

The spectral signature of leaf tissue is correlated with its photosynthetic pigment content, its cell anatomical structure, and its water content. Because VIs are associated with plant biophysical characteristics, they are related to many crop agronomic characteristics, such as leaf area (Viña et al., 2010), plant nutrient and health status (Cammarano et al, 2014; Feng et al., 2017), and soil physical and chemical characteristics (Bernardi et al., 2017). VIs are commonly used for spatial analysis of vegetation development and may therefore also aid in selecting management practices in cultivated areas.

Assuming that the crop vegetative status can vary spatially, mapping VIs is essential to identify homogeneous zones (HZs) that can differentiate intrinsic variations in these areas. Local changes in VI spatial distribution patterns together with analysis of other environmental parameters may therefore indicate the need of acting on possible causes of this variability. This should be performed by the adoption of site-specific management as a practice of precision agriculture.

Delimiting HZs of vegetative growth is particularly important for wine grape cultivars because their productive characteristics are affected by plant vigor. Delimiting HZs in vineyards therefore allows one to obtain grapes and wines of different qualities, depending on crop development and growth conditions. Trougtht & Bramley (2011) studied selective harvesting based on spatial and temporal variations

[1] FCA UNESP/ Botucatu - SP, Brasil.
[2] Georg-August-Universitat Gottingen, Gottingen, Germany.

Area Editor: Fabio Henrique Rojo Baio
Received in: 2-21-2019
Accepted in: 5-15-2019

in vine vegetative vigor, inferred from spectral reflectance measurements, and observed the influence of this variation on qualitative aspects of fruit maturation.

In delimiting HZs, each variable corresponds to a specific crop or field characteristic and represents a layer of information. Multivariate analysis methods may therefore be used to jointly evaluate the spatial distribution of several cultivated area characteristics, allowing the delimitation of HZs for several characteristics of interest. This type of approach was used by Aggelopooulou et al. (2013) to delimit HZ for soil properties, yield, and fruit quality in an apple orchard, considering spatial and temporal variations. Similarly, multivariate analysis applied to spatial interpolated data of different VIs may be used to identify variations in crop vegetative vigor that can describe the relationship between different aspects of the crop's spectral behavior. This methodology is particularly useful for the analysis of VI variations, used for delimitation of HZs, because different VIs may have different spatial distribution patterns in a given area, resulting in different HZ validation results. HZ validation is performed by identifying differences in the variables of interest between different HZs.

The aim of the present study was to characterize the spatial distribution of several VIs using geostatistics and define HZs representative of the vegetative status of Cabernet Franc and Cabernet Sauvignon vines using multivariate VI analysis.

MATERIAL AND METHOD

The study was performed at two commercial wine vineyards (*Vitis vinifera* L.), planted with cultivars Cabernet Franc (Area 1) and Cabernet Sauvignon (Area 2), in the municipality of Espírito Santo do Pinhal in the state of São Paulo, Brazil (Area 1: 22° 10' 41.11" S, 46° 42' 11.77" W; Area 2: 22° 10' 43.53" S, 46° 42' 14.69" W). Both Area 1 and Area 2 have an average altitude of 1,182 m and an area of 1.50 ha and 0.59 ha, respectively. The region's climate has been classified as B3rB'3a' (Rolim et al., 2007). The soil in both areas has been classified predominantly as eutrophic Tb Haplic Cambisol (Santos et al., 2018), with texture varying between loamy-sandy-clayey (Area 1) and sandy-clayey (Area 2).

Cultivars Cabernet Franc and Cabernet Sauvignon were grafted on Paulsen 1103 rootstocks, spaced 3.0 m between rows and 1.0 m between plants, trained in an unilateral Royat cordon system using a vertical trellis system. The areas were drip-irrigated, with two emitters per plant and at an average flow rate of 1.60 L h^{-1} per emitter. Irrigation management was based on replacement of crop evapotranspiration (ETc, mm day^{-1}).

The double pruning system (Regina et al., 2006) was used in the vineyards. Evaluation was based on reflectance (ρ) measurements, performed by proximal sensing at canopy height, followed by calculation of VIs, once during the grapevine cycle (November 8, 2017). Data for VI calculation were measured in the field using the Crop Circle portable system with an ACS-430 active sensor (Holland Scientific, Lincoln, USA). The sensor incorporates three optical measurement channels, simultaneously measuring crop spectral reflectance at 670 nm (ρ_R, red), 730 nm (ρ_{RE}, red edge), and 780 nm (ρ_{NIR}, near-infrared). The data were stored in a GeoSCOUT GLS-400 data logger (Holland Scientific, Lincoln, NE, USA). Data collection was performed by systematic sampling, moving the sensor along the whole length of the planting row. Planting rows were oriented northeast-southwest (NE-SW) in both areas, and had an average length 105.43 ± 26.85 m in Area 1 and 74.36 ± 24.40 m in Area 2. The sensor was placed at a height of approximately 0.30 m from the top of the plant canopy and set for 10 readings per second, resulting in an average of 8.11 ± 2.25 and 7.62 ± 0.32 ρ measurements per meter of plant row, and a total 38,402 and 14,461 sampling points, for Areas 1 and 2, respectively. The sampling points were simultaneously georeferenced with data collection, using a HiPer GGD Global Navigation Satellite System (GNSS) receiver (TOPCON, Pleasanton, USA), with the signal corrected by Real Time Kinematic (RTK). Data were acquired during the morning, between 12h:16 min and 14h:16 min UTC. The total operational time was approximately 0.40 and 1.07 h, assuming an average walking speed of 4.58 ± 0.55 and 4.73 ± 0.20 km h^{-1}, for Areas 1 and 2, respectively. The planting row layout in the study areas, which guided the ρ data collection, is presented in Figure 1.

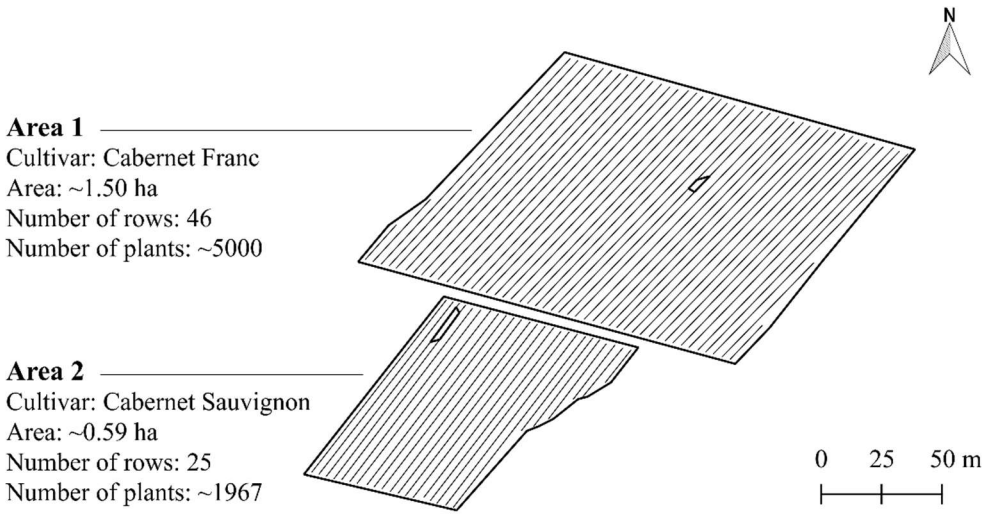

FIGURE 1. Representation of the perimeter and planting row layout of the study areas considered for reflectance (ρ) data acquisition. Reflectance was measured at three wavelengths, at canopy height, using the Crop Circle ACS-430 active sensor, and used to calculate VIs. The study areas were planted with Cabernet Franc and Cabernet Sauvignon vines.

The ρ measured at canopy height was used to calculate nine different VIs measured with the active sensor (Table 1).

TABLE 1. Vegetation indices (VIs) calculated from reflectance values measured using an ACS-430 sensor.

Abbreviation	Equation	Vegetation index
SRI	ρ_{NIR}/ρ_R	*Simple Ratio Index – Red*
ChlI	$(\rho_{NIR}/\rho_{RE}) - 1$	*Chlorophyll Index – Red Edge*
NDVI	$(\rho_{NIR} - \rho_R)/(\rho_{NIR} + \rho_R)$	*Normalized Difference Vegetation Index*
NDRE	$(\rho_{NIR} - \rho_{RE})/(\rho_{NIR} + \rho_{RE})$	*Normalized Difference Red Edge*
CCCI	$[(\rho_{NIR} - \rho_{RE})/(\rho_{NIR} + \rho_{RE})]/[(\rho_{NIR} - \rho_R)/(\rho_{NIR} + \rho_R)]$	*Canopy Content Chlorophyll Index*
NLI	$(\rho_{NIR}^2 - \rho_R)/(\rho_{NIR}^2 + \rho_R)$	*Non-Linear Vegetation Index*
RDVI	$(\rho_{NIR} - \rho_R)/(\rho_{NIR} + \rho_R)^{1/2}$	*Re-normalized Difference Vegetation Index*
MSR	$[(\rho_{NIR}/\rho_R) - 1]/[(\rho_{NIR}/\rho_R)^{1/2} - 1]$	*Modified Simple Ratio*
IPVI	$\rho_{NIR}/(\rho_{NIR} + \rho_R)$	*Infrared Percentage Vegetation Index*

A descriptive statistical analysis was performed on the ρ measured at the three wavelengths and the nine VIs calculated, which were summarized in measures of central tendency and dispersion, using the R 3.3.3. software (R Core Team, 2017). Relative dispersion was evaluated based on the coefficient of variation (CV), and classified as low (CV ≤ 15%), moderate (15 < CV ≤ 35%) or high (CV > 35%), according to Wilding (1985).

Spatial characterization, based on ρ and VI variation and distribution along the vineyard, was performed by geostatistical analysis, using the Vesper 1.6 software (Minasny et al., 2005). Geostatistical analysis was performed in two stages. First, semivariograms were fitted based on the assumption of the stationarity of the intrinsic hypothesis and of the semivariance calculation γ(h), according to [eq. (1)] as follows:

$$\gamma(h) = [1/2N(h)] \sum_{i=1}^{N} [Z(x_i) - Z(x_i - h)]^2 \quad (1)$$

Where,

N(h) is the number of measured value pairs, $Z(x_i)$ and $Z(x_i+h)$, separated by a vector h (Grego & Oliveira, 2015). Assuming the exponential model, theoretical semivariograms were fitted by the automatic fitting method using a moving window procedure (Haas et al., 1990), as recommended for large sampling densities (> 5000 points). The pre-selection of the exponential model was based on previous geostatistical analyses performed for characterization of the spatial distribution of VIs (particularly the normalized difference vegetation index - NDVI), measured by proximal sensing, for wine grape cultivars growing in areas adjacent to the present study areas. The evaluation of the fitting quality showed lower root mean square error (RMSE), which represents the average magnitude of the estimated error (Oliveira, 2015), for the exponential model compared to that of the remaining models evaluated (Gaussian and spherical). The exponential model for fitting of the theoretical semivariogram is described by [eq. (2)] as follows:

$$\gamma(h) = C_0 + C_1[1 - \exp(-3h/a)] \qquad 0 < h < d \quad (2)$$

Where,

γ(h) is the semivariance for the fitted model; C_0 and C_1 are the fitting parameters of the nugget and sill effect, respectively; *h* is the distance; *a* is the variogram range; and *d* is the maximum distance by which the semivariogram is defined (Grego & Oliveira, 2015). In the model selection options, the ratio between the number of value pairs and the semivariance standard deviation was used as a weighing factor when fitting the theoretical to the empirical semivariogram, using weighed non-linear regression.

The second stage of the geostatistical analysis consisted of spatial inference determined by interpolation of the ρ and VI values by ordinary kriging. Thematic maps were then generated by importing the interpolated data into a Geographic Information System (GIS), using the QGIS 2.18.17 software (QGIS Development Team, 2016). The intervals for each variable (ρ and VI) were categorized into three classes, adopting the Jenks Optimization method as classification rule, which minimizes the intrinsic differences and maximizes the differences between classes (Fraile et al., 2016). An explanation of the classification procedure used in building choropleth maps according to the Jenks Optimization, and its comparison to other methods, can be found in Ramos et al. (2016).

Using the interpolated VI values, a multivariate analysis was performed to delimit HZs, using two processes: principal component analysis (PCA), using the R 3.3.3 software (R Core Team, 2017), and clustering analysis of the scores of the selected principal components (PCs) using fuzzy k-means clustering (non-hierarchical iterative) in the FuzME 3.5 software (Minasny & McBratney, 2002). Notably, only PCs with an eigenvalue > 1 were selected (Tripathi et al., 2015). The optimal number of HZs was selected based on the fuzziness performance index (FPI) (Fridgen et al., 2004) and modified partition entropy (MPE) (Boydell & McBratney, 2002). FPI is a measure of the degree of separation between observations, i.e. between the interpolated data, and the clusters generated whereas MPE is a measure of the amount of disorganization between clusters (Fridgen et al., 2004). Clusters constituted by 2 to 5 HZs were tested and the ideal category size was chosen based on the lowest FPI and MPE. The lowest number of HZs resulting from VI clustering was also chosen based on the Wilks Lambda (Λ) (Wilks, 1932), which is the ratio between the cluster intrinsic and total variance.

Finally, the HZ classes were validated by comparing the means for each VI, calculated from a sample of ρ values from the original data set, by analysis of variance, using the Tukey test, at p≤0.05, applying the R 3.3.3 software (R Core Team, 2017).

RESULTS AND DISCUSSION

A numerical summary of the descriptive statistics for the set of observed ρ and calculated VI values is presented in Table 2. Regarding reflectance at each wavelength, the highest relative variability was observed for red (ρ_R) for both areas, as indicated by the CV (32.57% for Area 1 and 54.67% for Area 2). The CV was classified as moderate (15 < CV ≤ 35%) for Area 1 and high (CV > 35%) for Area 2. The ρ_R variability indicated high canopy discontinuity along the planting rows, given the variation in grapevines canopy density. This can be inferred because the canopy reflectance in the visible and near infrared regions is influenced by the amount of green tissue present (Amaral et al., 2015). In addition, because Area 2 presented a higher CV than Area 1, the relative variation was assumed to be higher for the Cabernet Sauvignon than for the Cabernet Franc vine cover, indicating a biomass decrease. For both areas, relative dispersion was lower for ρ_{RE} than for the remaining wavelengths, and was classified as low for both ρ_{RE} and ρ_{NIR} (CV ≤ 15%).

TABLE 2. Descriptive statistics for reflectance (ρ) and vegetation indices (VIs). Reflectance was measured at three wavelengths, at canopy height, using an ACS-430 active sensor. The study areas were planted with Cabernet Franc and Cabernet Sauvignon vines.

Variables	Mean	Maximum	Minimum	Amplitude	SD	CV(%)
Area 1 (Cabernet Franc)						
ρ_R	2.861	15.730	0.650	15.080	0.932	32.57
ρ_{RE}	20.380	24.500	17.470	7.030	0.588	2.88
ρ_{NIR}	34.247	53.820	24.830	28.990	2.144	6.26
SRI	12.735	68.274	1.615	66.659	2.901	22.78
ChlI	0.685	2.081	0.013	2.067	0.153	22.33
NDVI	0.846	0.971	0.235	0.736	0.047	5.52
NDRE	0.253	0.510	0.007	0.503	0.043	16.92
CCCI	0.298	0.757	0.028	0.729	0.047	15.74
NLI	0.995	0.999	0.952	0.048	0.002	0.21
RDVI	5.150	6.906	1.505	5.401	0.325	6.30
MSR	2.543	7.263	0.271	6.992	0.424	16.67
IPVI	0.923	0.986	0.618	0.368	0.023	2.53
Area 2 (Cabernet Sauvignon)						
ρ_R	2.971	23.030	0.560	7.280	1.624	54.67
ρ_{RE}	20.396	24.610	16.440	3.850	0.644	3.16
ρ_{NIR}	34.222	72.270	24.690	13.710	2.302	6.73
SIR	13.079	55.518	1.072	23.074	3.857	29.49
ChlI	0.683	3.396	0.003	0.978	0.164	24.03
NDVI	0.841	0.965	0.035	0.350	0.077	9.10
NDRE	0.252	0.629	0.002	0.276	0.046	18.35
CCCI	0.299	0.961	0.016	0.294	0.049	16.41
NLI	0.995	0.999	0.927	0.017	0.004	0.42
RDVI	5.125	8.101	0.240	2.889	0.482	9.40
MSR	2.571	6.451	0.035	3.414	0.571	22.20
IPVI	0.921	0.982	0.517	0.175	0.038	4.16

ρ_R, ρ_{RE}, ρ_{NIR}: reflectance at 670, 730 and 780 nm, respectively; SD: standard deviation.

The highest relative variation of VI was observed for SRI and ChlI, for both studied areas, but was classified as moderate (15 < CV ≤ 35%) in both cases. SRI and ChlI presented higher dispersion in Area 2 than in Area 1, similar to that observed for ρ_R. Because of its calculation equation, SRI was negatively correlated with ρ_R (670 nm) and positively correlated with ρ_{NIR} (780 nm), showing the same proportionality relative to canopy density. The low ρ_R together with high ρ_{NIR} therefore resulted in increased SRI and indicated areas in the vineyards with a lower predominance of empty spaces between plants and higher vegetative vigor. ChlI was negatively correlated with ρ_{RE} (730 nm), and together with high ρ_{NIR} (780 nm), indicated higher plant biomass. Notably, NLI was the VI with the lowest variation with relative dispersion classified as low (CV ≤ 15%) for both areas.

The spatial distributions of reflectance at the three wavelengths, measured using the ACS-430 sensor and VI calculated based on reflectance values, for Areas 1 and 2 are presented in Figures 2 and 3, respectively. Variations in the HZ spatial distribution pattern were observed for all variables, but the VIs were best correlated with the ρ at the wavelengths that were used in their calculation. Therefore, the canopy content chlorophyll index (CCCI), ChlI, and normalized difference red edge index (NDRE) were more negatively correlated with ρ_{RE} and ρ_{NIR} whereas the infrared percentage vegetation index (IPVI), modified simple ratio (MSR), NDVI, non-linear index (NLI), renormalized difference vegetation index (RDVI), and solar reflectance index (SRI) were more negatively correlated with ρ_R.

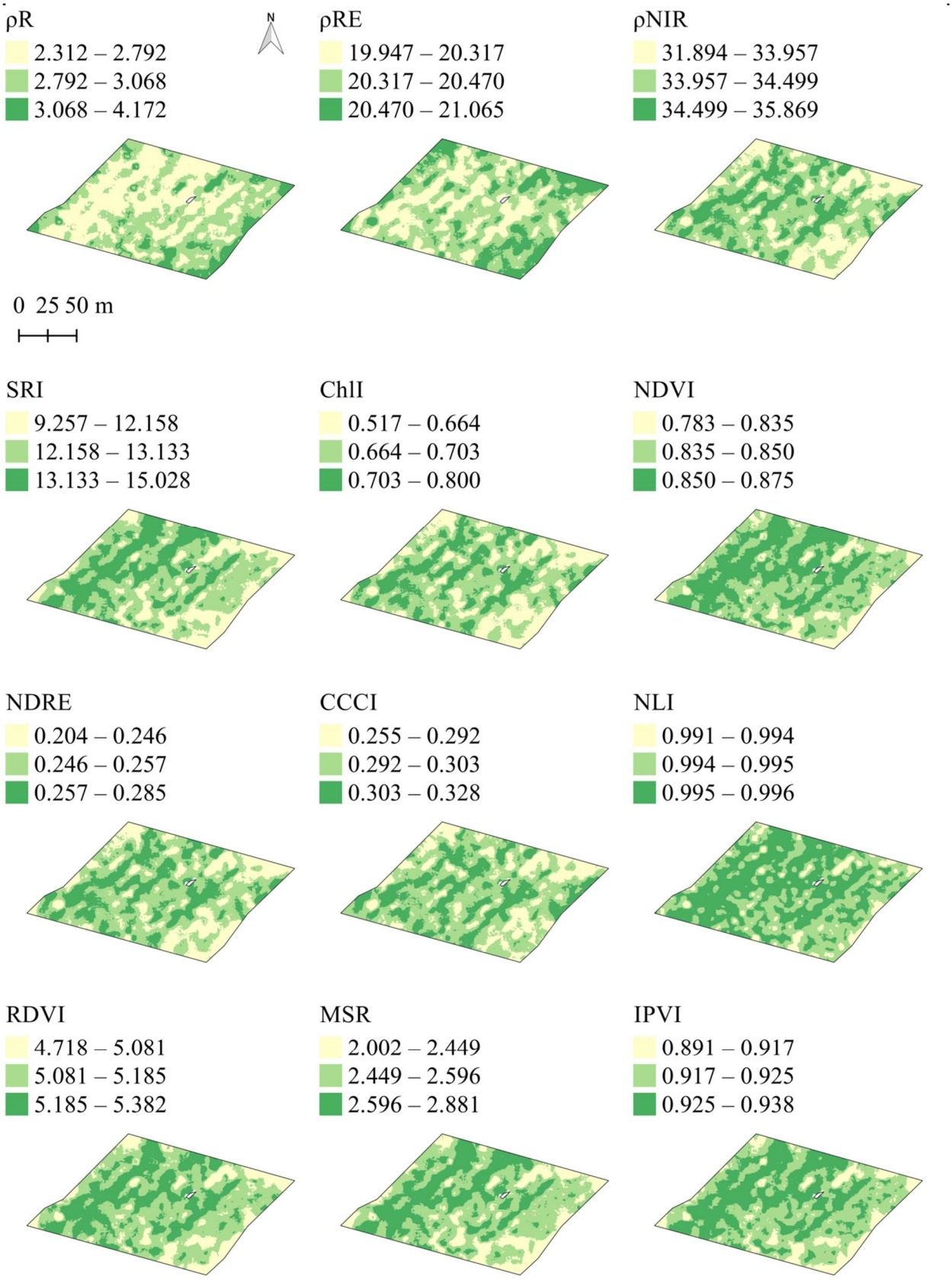

FIGURE 2. Spatial distribution of HZs for reflectance (ρ) and VIs for Cabernet Franc vines. Reflectance was measured at three wavelengths at canopy height using an ACS-430 active sensor.

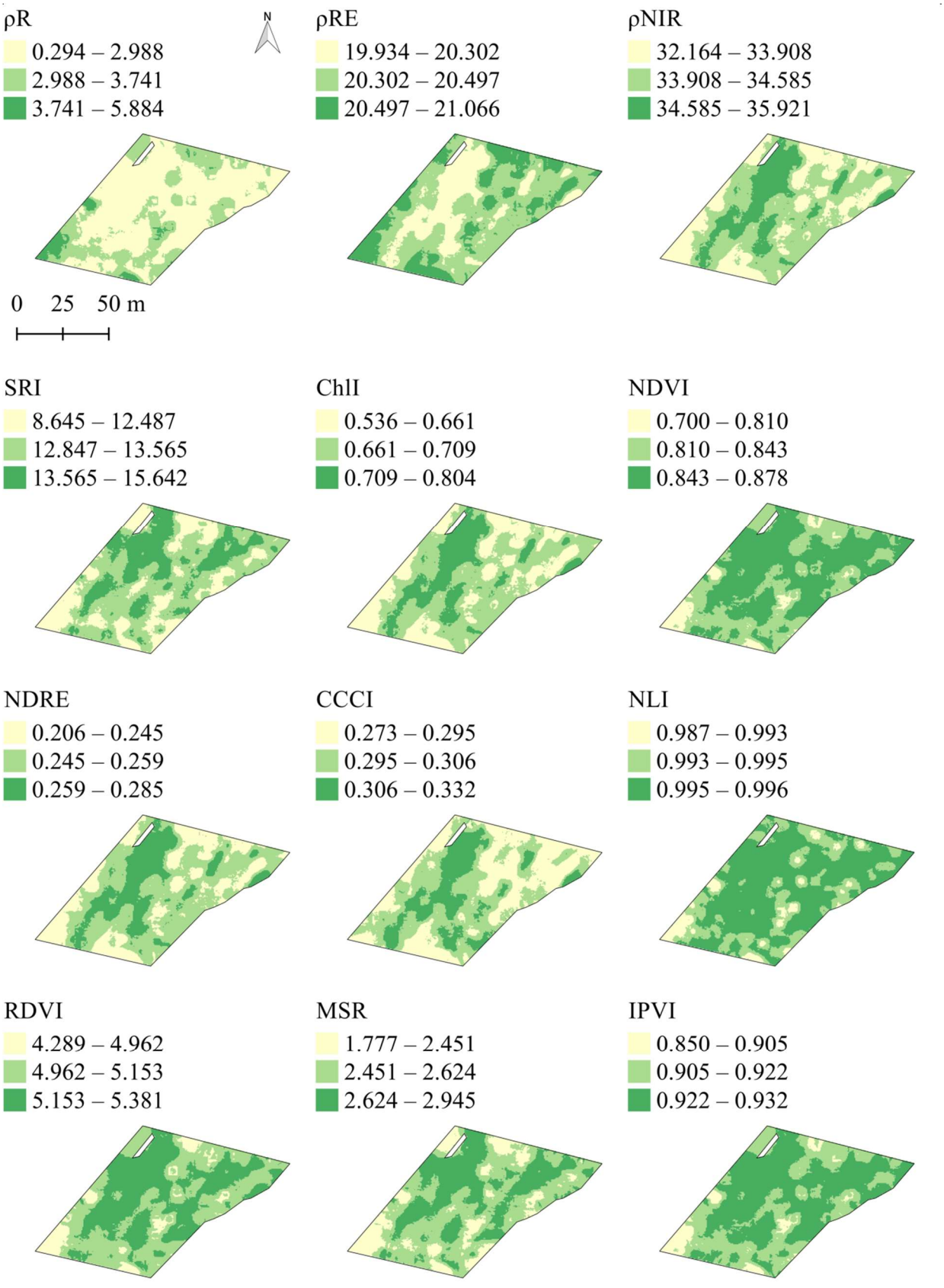

FIGURE 3. Spatial distribution of HZs for reflectance (ρ) and VIs for Cabernet Sauvignon vines. Reflectance was measured at three wavelengths at canopy height using an ACS-430 active sensor.

The inversely proportional relationship between VIs and ρ_R can be explained by the typical absorption spectrum of chlorophyll. Chlorophyll absorbs light more strongly in the blue (~430 nm) and red (~660 nm) range, being the least efficient pigment to absorb light in the middle range, reflecting green light (~550 nm) (Taiz & Zeiger, 2008). The relationship between reflectance, represented by the VI, and leaf chlorophyll content was demonstrated by Carmona et al. (2015) using spectra for several cultivated areas and by Kooistra & Clevers (2016) for potato (*Solanum tuberosum* L.) fields. However, Amaral et al. (2015) observed a higher correlation between sugarcane canopy reflectance, measured by proximal sensing, and biomass and no correlation with the relative chlorophyll concentrations. According to the authors, this relationship was explained by the plant population variability and the presence of gaps in the planting rows, which more pronouncedly affects the reflectance measurements. A similar case may occur in vineyards because of the shape of the training system, in response to the plant vegetative stage, and as a result of crop management practices, such as different types of green pruning (removing of leaves and branch tips) adopted during the crop cycle, which affect canopy density. Because of its applicability, VI remote sensing has been adopted to evaluate parameters related to vine vegetation status, namely to predict pruning weight (Dobrowski et al., 2003), estimate leaf area (Drissi et al., 2009), monitor leaf phenological development (Fraga et al., 2014), and estimate plant water status (Pôças et al., 2015).

The results of the PCA for the interpolated VI values mapped for both areas are presented in Table 3. Two PCs (PC1 and PC2) were selected for all cases, according to the selection criteria, because they presented an eigenvalue > 1.

TABLE 3. Principal component analysis for the vegetation indices (VIs), calculated based on reflectance (ρ), for the two study areas. Reflectance was measured at canopy height using an ACS-430 active sensor. The study areas were planted with Cabernet Franc and Cabernet Sauvignon vines.

Area - cv.	PC	Eigenvalue	Variance (%)	Accumulated variance (%)
1 - CF	PC1	7.33	81.47	81.47
	PC2	1.30	14.47	95.94
2 - CS	PC1	7.10	78.86	78.86
	PC2	1.43	15.88	94.74

		Principal Component Loading								
Area - cv.	PC	SRI	ChlI	NDVI	NDRE	CCCI	NLI	RDVI	MSR	IPVI
1 - CF	PC1	-0.939	-0.880	-0.934	-0.889	-0.703	-0.874	-0.988	-0.948	-0.937
	PC2	0.235	-0.465	0.315	-0.451	-0.702	0.264	0.017	0.257	0.317
2 - CS	PC1	-0.913	-0.878	-0.938	-0.896	-0.550	-0.876	-0.985	-0.943	-0.939
	PC2	-0.149	0.467	-0.308	0.431	0.825	-0.292	-0.091	-0.200	-0.309

cv.: cultivar; CF: Cabernet Franc; CS: Cabernet Sauvignon; PC: Principal Component

A large part of the data variance was explained by PC1, as indicated by the accumulated variance of 81.47% for Area 1 and 78.86% for Area 2. PC2 explained 14.47% and 15.88% of the total variance, and resulted in an accumulated variance of 95.94% and 94.74%, for Areas 1 and 2, respectively. PC1 and PC2 therefore explained most of the VI total variance for both areas.

Based on the PC loadings for both areas, PC1 represented most VI. CCCI was the VI with the highest loading, and the only one with high expression, in PC2, particularly for Area 2. A predominance of RDVI participation in PC1 was also observed, presenting a higher negative loading than that of the remaining components for both areas.

The results of the validation for selection of the ideal number of HZs, based on the FPI, MPE, and Λ for each category, are presented in Figure 4. The spatial distribution of the optimal number of HZs obtained by the clustering analysis of interpolated VI values is presented in Figure 5.

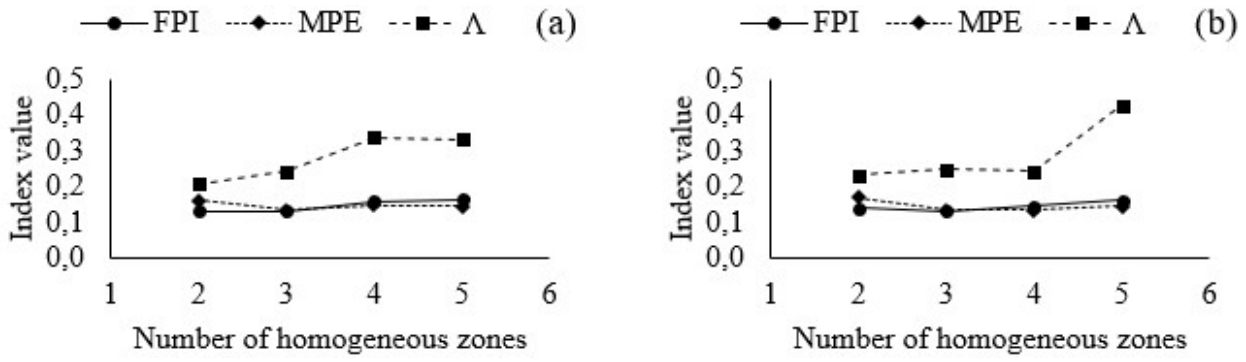

FIGURE 4. Fuzziness performance index (FPI), modified partition entropy (MPE), and Wilks Lambda (Λ) resulting from the clustering analysis of different VIs, calculated based on ρ, for two study areas. Reflectance was measured at canopy height, using an ACS-430 active sensor. The study areas were planted with Cabernet Franc and Cabernet Sauvignon vines.

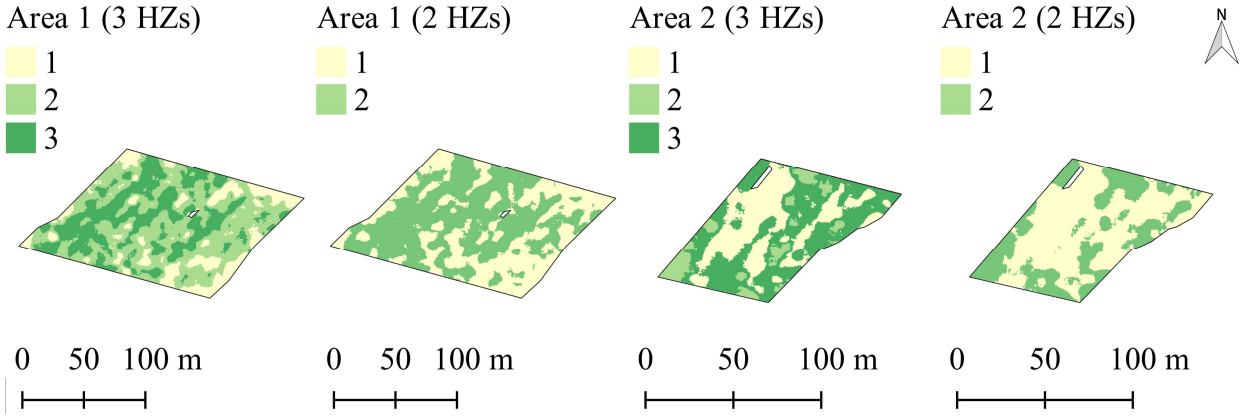

FIGURE 5. Spatial distribution resulting from the clustering analysis of VIs, calculated based on ρ, for two study areas. Reflectance was measured at canopy height, using an ACS-430 active sensor. The study areas were planted with Cabernet Franc and Cabernet Sauvignon vines.

For both areas, FPI and MPE were lower for the clustering of VIs into three HZs than for the remaining classes (0.131 and 0.135 for Area 1 and 0.130 and 0.133 for Area 2, respectively). However, the lowest Λ was observed for the clustering into two HZs (0.208 for Area 1 and 0.231 for Area 2). Therefore, based on FPI and MPE, three was considered the ideal number of HZs to represent the canopy spatial distribution, as indicated by the VIs. However, given the Λ values, VI clustering into two HZs was also adopted and used for practical purposes of area delimitation, because given the area extension, a higher fragmentation could make site-specific management operations in the vineyards impossible.

Based on the delimitation of vine canopy variability, the evaluation of environmental properties that affect the plant canopy characteristics, and monitoring of the temporal stability of these characteristics, differentiated management practices can be adopted within the context of precision viticulture. Plant vigor is particularly important in viticulture, because of the need of a balance between vegetative and reproductive development. Notably, vine physiological responses depend on environmental conditions and are affected by the adopted management practices (Steyn et al., 2016).

The analysis of vine vigor variability can also be used to guide more efficient sampling practices. The design of vegetative vigor HZs can therefore guide the evaluation of plant water status and productivity as determined by the number of grape bunches and the monitoring of grape quality and maturation.

The means of VIs, calculated from a sample of ρ values measured in points in each one of the HZs delimited by the clustering analysis, and the results of the analysis of variance for validation of the classification obtained by the clustering analysis, are presented in Table 4.

TABLE 4. Means and analysis of variance for the differentiation of classes of HZs of different VIs calculated based on ρ for the two study areas. Reflectance was measured at canopy height, using an ACS-430 active sensor. The study areas were planted with Cabernet Franc and Cabernet Sauvignon vines.

HZ	SIR	CHLI	NDVI	NDRE	CCCI	NLI	RDVI	MSR	IPVI
Area 1 (Cabernet Franc)									
1	11.410 c	0.616 b	0.836 c	0.235 b	0.281 b	0.995 c	5.035 c	2.370 c	0.918 c
2	12.689 b	0.654 b	0.852 b	0.246 b	0.289 b	0.995 b	5.149 b	2.556 b	0.926 b
3	14.066 a	0.722 a	0.866 a	0.265 a	0.305 a	0.996 a	5.288 a	2.747 a	0.933 a
Pr>F	$4.38\ 10^{-9}$	$5.80\ 10^{-6}$	$1.92\ 10^{-8}$	$6.55\ 10^{-6}$	$9.99\ 10^{-4}$	$2.24\ 10^{-9}$	$5.55\ 10^{-10}$	$5.92\ 10^{-9}$	$1.92\ 10^{-8}$
1	11.137 b	0.618 b	0.825 b	0.234 b	0.282 a	0.994 b	4.985 b	2.311 b	0.913 b
2	13.384 a	0.689 a	0.857 a	0.255 a	0.298 a	0.996 a	5.210 a	2.646 a	0.929 a
Pr>F	$1.24\ 10^{-3}$	$4.79\ 10^{-2}$	$2.58\ 10^{-3}$	$3.46\ 10^{-2}$	$1.48\ 10^{-1}$	$2.92\ 10^{-3}$	$3.41\ 10^{-3}$	$1.39\ 10^{-3}$	$2.59\ 10^{-3}$
Area 2 (Cabernet Sauvignon)									
1	14.321 a	0.725 a	0.865 a	0.265 a	0.306 a	0.996 a	5.284 a	2.766 a	0.932 a
2	11.563 b	0.668 a	0.827 b	0.249 a	0.303 a	0.994 b	5.040 b	2.362 b	0.913 a
3	13.515 a	0.675 a	0.854 a	0.250 a	0.292 a	0.995 a	5.179 ab	2.649 a	0.927 a
Pr>F	$3.55\ 10^{-3}$	$2.02\ 10^{-1}$	$2.96\ 10^{-3}$	$2.04\ 10^{-1}$	$4.26\ 10^{-1}$	$4.42\ 10^{-3}$	$4.22\ 10^{-3}$	$2.97\ 10^{-3}$	$2.95\ 10^{-3}$
1	13.446 a	0.657 a	0.855 a	0.246 a	0.288 a	0.995 a	5.163 a	2.641 a	0.927 a
2	11.942 a	0.680 a	0.830 a	0.252 a	0.305 a	0.994 a	5.070 a	2.412 a	0.915 a
Pr>F	9.70^{-2}	4.57^{-1}	$5.54\ 10^{-2}$	$4.97\ 10^{-1}$	$1.09\ 10^{-1}$	$7.47\ 10^{-2}$	$2.22\ 10^{-1}$	$8.16\ 10^{-2}$	$5.52\ 10^{-2}$

HZ: homogeneous zones. Means with the same letter are not statistically significantly different according to the Tukey test, at p≤0.05.

For Area 1, considering the division of spatial variability into two categories, significant differences between the HZs were observed for all VIs except CCCI, confirming the differentiation between the HZ delimited by the clustering analysis. In the area cultivated with Cabernet Franc, the highest average VIs were observed for HZ 3, classified as presenting higher canopy density than HZs 1 and 2. For Area 2, considering three HZs, significant differences between HZs were observed only for SRI, NDVI, NLI, RDVI and MSR. No significant differences in these indices were observed between HZs 1 and 3 whereas they were significantly lower for HZ 2. However, for Area 2, categorization into two HZs resulted in no significant differences in any VIs included in the clustering analysis. Dividing the area with cv. Cabernet Sauvignon into only two categories was therefore not sufficiently sensitive to identify the spatial variability of the canopy density. Despite of this result, the set of analyses performed in the present study supported the spatial evaluation of overall vegetation status of vineyards based on the variations in canopy reflectance measured by proximal sensing.

CONCLUSIONS

The multivariate analysis of vegetation indices allowed the delimitation of HZs of vegetative vigor, with different patterns of spatial distribution, in Cabernet Franc and Cabernet Sauvignon vineyards.

Differences between HZs were confirmed by analysis of variance of the VIs used for their validation, for the clustering into two or three homogeneous zones for Area 1 and three homogeneous zones for Area 2.

ACKNOWLEDGMENTS

The authors would like to thank the Coordenação de Aperfeiçoamento de Pessoal de Nível Superior (CAPES) for their scholarship, the Conselho Nacional de Desenvolvimento Científico e Tecnológico (CNPq) for their scholarship and project funding, and Vinícola Guaspari for the use of the study area and support during the study.

REFERENCES

Aggelopooulou K, Castrignanò A, Gemtos T, De Benedetto D (2013) Delineation of management zones in an apple orchard in Greece using a multivariate approach. Computers and Electronics in Agriculture 90:119-130. DOI: https://doi.org/10.1016/j.compag.2012.09.009

Amaral LR, Molin JP, Portz G, Finazzi FB, Cortinove L (2015) Comparison of crop canopy reflectance sensors used to identify sugarcane biomass and nitrogen status. Precision Agriculture 16:15-28. DOI: https://doi.org/10.1007/s11119-014-9377-2

Bernardi ACC, Grego CR, Andrade RG, Rabello LM, Inamasu RY (2017) Spatial variability of vegetation index and soil properties in an integrated crop-livestock system. Revista Brasileira de Engenharia Agrícola e Ambiental 21(8):513-518. DOI: https://doi.org/10.1590/1807-1929/agriambi.v21n8p513-518

Boydell B, McBratney AB (2002) Identifying potential within-field management zones from cotton-yield estimates. Precision Agriculture 3:9-23. DOI: https://doi.org/10.1023/A:1013318002609

Cammarano D, Fitzgerald GJ, Casa R, Basso B (2014) Assessing the robustness of vegetation indices to estimate wheat N in Mediterranean environments. Remote Sensing 6(4):2827-2844. DOI: https://doi.org/10.3390/rs6042827

Carmona F, Rivas R, Mora DCF (2015) Vegetation Index to estimate chlorophyll content from multispectral remote sensing data. European Journal of Remote Sensing 48(1):319-326. DOI: https://doi.org/10.5721/EuJRS20154818

Dobrowski SZ, Ustin SL, Wolpert JA (2003) Grapevine dormant pruning weight prediction using remotely sensed data. Australian Journal of Grape and Wine Research 9(3):177–182. DOI: https://doi.org/10.1111/j.1755-0238.2003.tb00267.x

Drissi R, Goutouly JP, Forget D, Gaudillere JP (2009) Nondestructive measurement of grapevine leaf area by ground Normalized Difference Vegetation Index. Agronomy Journal 101(1):226-231. DOI: https://doi.org/10.2134/agronj2007.0167

Feng W, Qi S, Heng Y, Zhou Y, Wu Y, Liu W, He L, Li X (2017) Canopy vegetation indices from in situ hyperspectral data to assess plant water status of winter wheat under powdery mildew stress. Frontiers in Plant Science 8:1-12. DOI: https://doi.org/10.3389/fpls.2017.01219

Fraga H, Amraoui M, Malheiro AC, Moutinho-Pereira J, Eiras-Dias J, Silvestre J, Santos JA (2014) Examining the relationship between the Enhanced Vegetation Index and grapevine phenology. European Journal of Remote Sensing 47(1):753-771. DOI: https://doi.org/10.5721/EuJRS20144743

Fraile A, Larrodé E, Magreñán ÁA, Sicilia JA (2016) Decision model for siting transport and logistic facilities in urban environments: A methodological approach. Journal of Computational and Applied Mathematics 291:478-487. DOI: https://doi.org/10.1016/j.cam.2014.12.012.

Fridgen JJ, Kitchen NR, Sudduth KA, Drummond ST, Wiebold WJ, Fraisse CW (2004) Management zone analyst (MZA): software for subfield management zone delineation. Agronomy Journal 96(1):100-108. DOI: https://doi.org/10.2134/agronj2004.0100

Grego CR, Oliveira RO (2015) Conceitos básicos da geoestatística. In: Oliveira RO, Grego CR, Brandão ZN. Geoestatística aplicada na Agricultura de Precisão utilizando o Vesper. Embrapa Solos, p41-62.

Haas TC (1990) Kriging and automated variogram modeling within a moving window. Atmospheric Enviroment. Part A. General Topics 24(7):1759-1769. DOI: https://doi.org/10.1016/09601686(90)90508-K

Kooistra L, Clevers JGPW (2016) Estimating potato leaf chlorophyll content using ratio vegetation indices. Remote Sensing Letters 7(6):611-620. DOI: https://doi.org/10.1080/2150704X.2016.1171925

Minasny B, McBratney AB (2002) FuzME Version 3.5. Sydney, Australian Centre for Precision Agriculture, The University of Sydney.

Minasny B, McBratney AB, Whelan BM (2005) Vesper version 1.62. Sydney, Australian Centre for Precision Agriculture, The University of Sydney.

Oliveira RO (2015) Modelagem de variogramas. In: Oliveira RO, Grego CR, Brandão ZN. Geoestatística aplicada na Agricultura de Precisão utilizando o Vesper. Embrapa, p83-92.

Payero JO, Neale CMU, Wright JL (2004) Comparison of eleven vegetation indices for estimating plant height of alfalfa and grass. Applied Engineering in Agriculture 20(3):385-393. DOI: https://doi.org/10.13031/2013.16057

Pôças I, Rodrigues A, Gonçalves S, Costa PM, Gonçalves I, Pereira LS, Cunha M (2015) Predicting grapevine water status based on hyperspectral reflectance vegetation indices. Remote Sensing 7(12):16460-16479. DOI: https://doi.org/10.3390/rs71215835

QGIS Development Team (2016) QGIS Geographic Information System. Open Source Geospatial Foundation Project. Available: http://qgis.osgeo.org/.

R Core Team (2017) R: A language and environment for statistical computing. R Foundation for Statistical Computing. Available: https://www.R-project.org/.

Ramos APM, Marcato Junior J, Decanini, MMS, Pugliesi, EA, Oliveira, RF, Paranhos Filho, AC (2016) Avaliação qualitativa e quantitativa de métodos de classificação de dados para o mapeamento coroplético. Revista Brasileira de Cartografia 3(68):609-629.

Regina MA, Amorim DA, Favero AC, Mota RV, Rodrigues DJ (2006) Novos pólos vitícolas para produção de vinhos finos em Minas Gerais. Informe Agropecuário 27(234):111-118.

Rolim GS, Camargo MBP, Lima DG, Moraes JFL (2007) Classificação Climática de Köppen e de Thornthwaite e sua Aplicabilidade na determinação de zonas agroclimáticas para o estado de São Paulo. Bragantia 66(4):711-720. DOI: http://dx.doi.org/10.1590/S0006-87052007000400022

Santos HG dos, Jacomine PKT, Anjos LHC dos, Oliveira VA de, Lumbreras JF, Coelho MR, Almeida JA de, Araujo Filho JC de, Oliveira JB de, Cunha TJF (2018) Sistema brasileiro de classificação de solos. Brasília, Embrapa. 5 ed. 356p.

Steyn J, Aleixandre-Tudó J, Aleixandre JL (2016) Grapevine vigour and within-vineyard variability: A review. International Journal of Scientific & Engineering Research 7:1056-1065.

Taiz L, Zeiger E (2008) Fisiologia vegetal. Porto Alegre, Artmed, v.3, 819p.

Tripathi R, Nayak AK, Shahid M, Lal B, Gautam P, Raja R, Mohanty S, Kumar A, Panda BB, Sahoo RN (2015). Delineation of soil management zones for a rice cultivated area in eastern India using fuzzy clustering. Catena 133:128-136. DOI: https://doi.org/10.1016/j.catena.2015.05.009

Trought MCT, Bramley RGV (2011) Vineyard variability in Marlborough, New Zealand: characterizing spatial and temporal changes in fruit composition and juice quality in the vineyard. Australian Journal of Grape and Wine Research 17(1):79-89. DOI: https://doi.org/10.1111/j.1755-0238.2010.00120.x

Viña A, Gitelson AA, Nguy-Robertson A, Peng Y (2010) Comparison of different vegetation indices for the remote assessment of green leaf area index of crops. Remote Sensing of Environment 115(12):3468-3478. DOI: https://doi.org/10.1016/j.rse.2011.08.010

Wilding LP (1985) Spatial variability: its documentation, accommodation, and implication to soil surveys. In: Nielsen DR, Bouma J (ed). Soil spatial variability. Pudoc, p166-194.

Wilks SS (1932) Certain Generalizations in the Analysis of Variance. Biometrika 24(3):471-494.